



**HAL**  
open science

## Modeling control valves in water distribution systems using a continuous state formulation

Olivier Piller, Jakobus Ernst van Zyl

► **To cite this version:**

Olivier Piller, Jakobus Ernst van Zyl. Modeling control valves in water distribution systems using a continuous state formulation. *Journal of Hydraulic Engineering*, 2014, 140 (11), 04014052, 9 p. 10.1061/(ASCE)HY.1943-7900.0000920 . hal-01111075

**HAL Id: hal-01111075**

**<https://hal.science/hal-01111075>**

Submitted on 29 Jan 2015

**HAL** is a multi-disciplinary open access archive for the deposit and dissemination of scientific research documents, whether they are published or not. The documents may come from teaching and research institutions in France or abroad, or from public or private research centers.

L'archive ouverte pluridisciplinaire **HAL**, est destinée au dépôt et à la diffusion de documents scientifiques de niveau recherche, publiés ou non, émanant des établissements d'enseignement et de recherche français ou étrangers, des laboratoires publics ou privés.

1 **Modeling Control Valves in Water Distribution Systems Using a**  
2 **Continuous State Formulation**

3 by Olivier Piller<sup>1</sup> and Jakobus E. van Zyl<sup>2</sup> M.ASCE  
4

5 **ABSTRACT**

6 Control valves are commonly used for the operation of water distribution systems. Modeling  
7 these devices typically requires that their operating states are known, or that a  
8 computationally expensive search is undertaken over all possible operating states. This paper  
9 presents a novel method of modeling control valves (including flow control, pressure  
10 sustaining, pressure reducing and check valves) in extended-period simulations of water  
11 distribution systems. Instead of the normal discrete control problem formulation, it is  
12 approached with the Karush-Kuhn-Tucker equations for an optimization problem with  
13 constraints.

14  
15 The proposed method does not pre-require the operating state (open, closed, active) of each  
16 valve to be determined, as this is done implicitly. Pipe and valve flow rates and nodal heads  
17 are determined by (1) minimizing deviations from targets at control valves and (2) satisfy the  
18 state equations (conservation of mass and energy) by solving a constrained least-square  
19 problem.

20

---

<sup>1</sup> Research Scientist, Networks, water treatment and water quality Research Unit, Irstea, Bordeaux regional center, F-33612 Cestas France, email: [olivier.piller@irstea.fr](mailto:olivier.piller@irstea.fr)

<sup>2</sup> Associate Professor, Department of Civil Engineering, University of Cape Town, South Africa, email: [kobus.vanzyl@uct.ac.za](mailto:kobus.vanzyl@uct.ac.za)

21 Sensitivity equations with respect to the control variables (valve settings) are derived from  
22 the state equations, and the control variables are updated using Levenberg-Marquardt  
23 iterations. The results of simple problems and case studies are presented to demonstrate the  
24 effectiveness of the approach.

25 **Keywords:** Water distribution systems; Hydraulic models; Control valves; Algorithms;  
26 Least-squares optimization; Penalty method; Flow control; Pressure control

27

## 28 INTRODUCTION

29 Water distribution systems have to provide a high level of service under widely varying  
30 conditions. To achieve this, engineers often employ control valves to manage flows and  
31 pressures. Control valves can operate mechanically (such as check valves) or through  
32 hydraulic circuits (such as flow control and pressure regulating valves), and can be controlled  
33 by local conditions or an external signal.

34

35 The common algorithms used for modeling the hydraulics of a water distribution system do  
36 not model the time-varying behavior of the system continuously, but calculate snapshots of  
37 the system's hydraulic state at certain points in the simulation period. At each time step, the  
38 snapshot solver has to solve the hydraulic network equations while simultaneously  
39 calculating the settings of all the control valves in the system. Tank levels are updated  
40 between snapshot simulations using a simple Euler integration scheme.

41

42 The commonly used open source software, Epanet (Rossman, 2000), uses a set of control  
43 rules to calculate control valve settings. Although the Epanet method works well in practice  
44 and is widely accepted in the hydraulic modeling community, there is no guarantee that its  
45 heuristic algorithm will be able to find the correct control valve settings in all cases. In fact,

46 Simpson (1999) illustrated this through a number of control valve problems for which the  
47 Epanet hydraulic engine could not find a solution, or produced incorrect results.

48

49 Alternative methods for modeling control valves have developed in recent years. Piller and  
50 Bremond (2001) proposed a least-squares global optimization approach to determine the  
51 control valve state by minimizing the differences between the target settings and calculated  
52 values. Piller *et al.* (2005) applied the same optimization framework with an attempt to  
53 model time-varying behavior of the system continuously using slow transients (or rigid  
54 column without water hammer). This allowed them to model the continuous changes in the  
55 system state until an equilibrium (steady) state is achieved. The reaction speed of the control  
56 valve can be incorporated in the calculations by adding a constraint in the optimization  
57 solver. The authors noted that certain solutions that are infeasible using a demand-driven  
58 approach are in fact possible in real life, and can be solved correctly if a pressure-driven  
59 approach is followed.

60

61 Deuerlein *et al.* (2005) proposed a method based on Nash Equilibrium to determine the  
62 correct settings of pressure control valves. The valve head losses were taken as optimization  
63 variables and were estimated with a gradient-based algorithm that minimizes the  
64 corresponding convex variational problem. This method simultaneously solves as many  
65 constrained convex minimization problems as the number of pressure regulating valves plus  
66 one. The derived system is composed of the steady state equations (reduced to the loop  
67 energy balances) with one additional equation for each pressure regulating valve and  
68 complementary slackness condition. This system employs nonnegative Lagrange multipliers  
69 and its Jacobian is non-symmetrical, which may lead to a reduced solving efficiency. This  
70 reflects the fact that the system is not derived from a single optimization problem. It is worth

71 noting that the authors found their method to be robust and to produce good results based on  
72 several example problems. In a further paper, Deuerlein *et al.* (2008) used the same approach,  
73 but with the residual squared between the predicted value and the target value. This  
74 represents a more direct objective function similar to that used by Piller and Bremond (2001).  
75 Moreover, the authors described some simple examples for which no solutions or no unique  
76 solutions could be found.

77  
78 Another method to handle flow control and check valves was proposed by Deuerlein *et al.*  
79 (2009). They use the content and co-content theory to define conditions that guarantee the  
80 existence and uniqueness of the solution before simultaneously solving the network  
81 hydraulics and valve settings. Subdifferential analysis is used to deal with the non-  
82 differentiable flow versus headloss relationships of flow control and check valves, and the  
83 combined equations are solved as a constrained nonlinear programming problem. An  
84 interesting result was the interpretation of the flow rate inequality multiplier as the head loss  
85 over the flow control valve.

86  
87 In this study, different approaches are used to solve flow and pressure control valves in a  
88 hydraulic network. Flow control valves are handled by applying an external penalty function  
89 to the valve's headloss equation in the vicinity of the valve setting. Check valves are handled  
90 as special flow control valves with a minimum flow rate setting of zero. The flow control  
91 valves are then solved with the other network hydraulic equations using a standard network  
92 solver. Pressure control valves are solved externally to the hydraulic solver by employing a  
93 Newton Projection Minimization algorithm, for which global convergence is guaranteed.

94

95 An overview of the snapshot hydraulic equations is presented before describing the proposed  
96 algorithms for handling flow and pressure control valves. The proposed method is illustrated  
97 on a number of example problems for which Epanet is not currently able to find correct  
98 solutions.

99

## 100 **HYDRAULIC MODEL**

101 *Hydraulic equations.* Equations describing the hydraulics of water distribution systems are  
102 based on the principles of conservation of mass and energy for an incompressible fluid. These  
103 equations are solved to obtain the unknown flow rates in pipes, and hydraulic heads at nodes.

104 The hydraulic network equations are described by:

$$105 \left\{ \begin{array}{l} \mathbf{A}\mathbf{Q}^* + \mathbf{d} = \mathbf{0}_{nu} \\ \mathbf{h}^* - \mathbf{A}^T \mathbf{H}^* - \mathbf{A}_f^T \mathbf{H}_f = \mathbf{0}_{np} \\ \mathbf{h}^* = \mathbf{h}(\mathbf{Q}^*, \mathbf{r}) \end{array} \right. \quad (14)$$

106 Where  $\mathbf{Q}^*$  is the vector of link flowrates with size  $np$  (number of links),  $\mathbf{d}$  the vector of nodal  
107 demands with size  $nu$  (number of unknown-head nodes),  $\mathbf{A}$  an  $nu \times np$  incidence matrix  
108 representing unknown-head node connectivity,  $\mathbf{A}_f$  an  $nf$  (number of fixed-head nodes)  $\times np$   
109 incidence matrix of fixed-head nodes,  $\mathbf{H}^*$  the vector of hydraulic heads for the unknown-head  
110 nodes,  $\mathbf{H}_f$  the vector of hydraulic heads for the fixed-head nodes,  $\mathbf{h}^*$  is a vector of link head  
111 losses.  $A_{ij} = +1$  if the pipe  $j$  leaves node  $i$  and  $i$  is an unknown head node;  $A_{ij} = -1$  if it enters  
112 node  $i$  and  $i$  is an unknown head node; and  $A_{ij} = 0$  otherwise. The same definition applies to  
113  $\mathbf{A}_f$  but with  $i$  a fixed head node. The first two equations describe the conservation of mass and  
114 energy respectively, and are linear. The last is a nonlinear equation that describes the  
115 relationship between the link flow rates and head losses, typically based on the Darcy-  
116 Weisbach or still Hazen-Williams formulae.

Code de champ modifié

Mis en forme : Police :12 pt, Ne pas  
vérifier l'orthographe ou la grammaire

117

118 *Solving the hydraulic equations.* Various methods have been proposed for solving water  
119 distribution system hydraulics. The first Loop method proposed by Cross (1936) updates the  
120 value of loop flow rates for the corresponding loop energy equation subject while fixing all  
121 other flow rates (a similar Node method was also proposed by Cross). It can be shown  
122 (Piller, 1995) that the Hardy Cross Loop method corresponds to a cyclic relaxation for the  
123 minimization of an energy function. The convergence of the latter can be drastically  
124 improved by simultaneously considering all the loops and nodes.

125

126 Subsequently, several Newton-Raphson based algorithms have been proposed. These  
127 algorithms may be classified as:

128 • Nodal methods, which are based on the nodal mass balances and describe the system  
129 state with head variables, e.g. (Chandrashekar and Stewart 1975; Lam and Wolla  
130 1972; Martin and Peters 1963).

131 • Loop or simultaneous path methods, which are based on loop energy balances and  
132 describe the system state with loop flow rate variables, e.g. (Carpentier *et al.*, 1985;  
133 Epp and Fowler 1970).

134 • The Linear method proposed by Wood and Charles (1972), which is based on mass  
135 and energy balances and describes the system with link flow rate variables.

136 • Hybrid methods, which are based on mass and energy balances and describe the  
137 system with both link flow rates and nodal head variables, e.g. (Carpentier *et al.*,  
138 1985; Todini and Pilati, 1988; Piller 1995).

139

140 The Loop, Linear and Hybrid method classes result in equations that are the best conditioned  
141 for fast convergence (they converge in the same number of iterations from the same starting

142 point), but the Hybrid method generally has fewer computational overheads than the other  
143 two methods, and is thus preferred. The Global Gradient Algorithm method by Todini and  
144 Pilati (1988) was implemented in the public domain Epanet software (Rossman 2000), which  
145 has become the standard method used in research and industry. Alternative Hybrid  
146 formulations are employed in software packages such as Piccolo (2013) and Porteau (2013).  
147 A problem with the Newton-Raphson based algorithms is that the global convergence of the  
148 method is only guaranteed if the initial solution is sufficiently close to the final solution (see  
149 e.g. the global damped Newton theorem in Ortega and Rheinboldt; 1970).

150

151 For global convergence to be guaranteed, it is necessary to adopt an optimization approach.  
152 Such formulations were proposed by Collins *et al.* (1978), Carpentier *et al.* (1985) and Piller  
153 (1995). An optimization approach allows correction made to the solution at each iteration to  
154 be tested for effectiveness, thus allowing numerical instabilities to be avoided. In addition,  
155 the existence and uniqueness of a solution to the equations can be proven, and thus  
156 convergence on a unique solution is guaranteed.

157

158 The proposed hydraulic solver is derived from the Content formulation by Collins, which  
159 describes the principle of least action for the hydraulic network, and can be written as:

160

$$\begin{aligned} \min_{\mathbf{Q}} f(\mathbf{Q}) &= \mathbf{Q}^T \bar{\mathbf{h}}(\mathbf{Q}) - \mathbf{Q}^T \mathbf{A}_f^T \mathbf{H}_f \\ \text{subject to } -\mathbf{A}\mathbf{Q} - \mathbf{d} &= \mathbf{0}_{nu} \end{aligned}$$

(22)

Code de champ modifié

Mis en forme : Police :12 pt, Ne pas vérifier l'orthographe ou la grammaire

161 Where  $f(\mathbf{Q})$  is called the Content function of the system. The units of the Content function  
162 are that of power per unit weight. It is expressed as the sum of two terms with the first term  
163 representing the power dissipated in the network to reach the final steady state and the second  
164 the external power available to the system.  $\mathbf{Q}$  is a vector of the link flowrates that complies



165 with the conservation of mass, but not necessarily with the conservation of energy (i.e. the  
166 link flowrates in the solver before convergence has been achieved).  $\bar{\mathbf{h}}$  is the vector of  
167 average headlosses between flowrates of zero to  $\mathbf{Q}$  and its  $i^{\text{th}}$  component is:

168 
$$\bar{h}_i(Q_i) = (1/Q_i) \int_0^{Q_i} h_i(u) du, \quad Q_i \neq 0 \quad \text{and} \quad \bar{h}_i(0) = 0$$

Code de champ modifié

Code de champ modifié

169  $\mathbf{Q}^*$  is used for the correct values of the flowrates after convergence (that complies with both  
170 mass and energy balance). Thus  $f(\mathbf{Q})$  is at a minimum when  $\mathbf{Q} = \mathbf{Q}^*$ .

171

172 Moreover, the headloss vector function  $\mathbf{h}$  is modified near zero to ensure that  $f(\mathbf{Q})$  is strongly  
173 convex and twice continuously differentiable. The modification is required to ensure that the  
174 first derivative of the headloss function does not become zero at a flowrate of zero ó for  
175 details, see Piller (1995). This smoothing process is not necessary to guarantee the existence  
176 and uniqueness of the solution, but avoids numerical problems experienced by hydraulic  
177 solvers when flows in pipes are close to zero (all solver algorithms have to deal with this  
178 problem in some way).

179

180 The Content model minimization problem (2) is solved with a Lagrange-Newton method that  
181 is obtained by applying a Newton method to find a saddle point of the problem Lagrangian.  
182 At each iteration, updated heads and flowrates, as well as the Content function are calculated.  
183 If the descent criterion (similar to the Wolfe conditions) is not satisfied (i.e. the Content  
184 function does not decrease sufficiently), the flowrate adjustment is diminished by a factor  $\rho_k$   
185 to ensure that global minimum of the Content function is found. At each iteration, the  
186 updated heads and flowrates are calculated by:

187

$$\begin{aligned}\mathbf{H}^{k+1} &= (\mathbf{A}\mathbf{D}_k^{-1}\mathbf{A}^T)^{-1} [\mathbf{A}\mathbf{D}_k^{-1} \{ \mathbf{h}(\mathbf{Q}^k) - \mathbf{A}_f^T \mathbf{H}_f \} - \{ \mathbf{A}\mathbf{Q}^k + \mathbf{d} \}] \\ \mathbf{Q}^{k+1} &= \mathbf{Q}^k - \rho_k \mathbf{D}_k^{-1} [\mathbf{h}(\mathbf{Q}^k) - \mathbf{A}_f^T \mathbf{H}_f - \mathbf{A}^T \mathbf{H}^{k+1}]\end{aligned}$$

(33)

Code de champ modifié

Mis en forme : Police :12 pt, Ne pas vérifier l'orthographe ou la grammaire

188 with  $\mathbf{D}_k = \mathbf{D}(\mathbf{Q}^k) = \partial_{\mathbf{Q}} \mathbf{h}(\mathbf{Q}^k)$  the Jacobian matrix of  $\mathbf{h}$  in  $\mathbf{Q}^k$  and  $\mathbf{A}\mathbf{D}_k^{-1}\mathbf{A}^T$  is a symmetric,  
189 positive definite Jacobian matrix associated to the unknown head update.

190

191 A convergence criterion on the energy balance on the pipes is used by stopping when

192  $\max_i \{ (\mathbf{h}(\mathbf{Q}^k) - \mathbf{A}_f^T \mathbf{H}_f - \mathbf{A}^T \mathbf{H}^{k+1})_i, i=1, \dots, n_p \} \leq \varepsilon$ , with a small value.

193

## 194 PROPOSED MODEL FOR FLOW AND PRESSURE REGULATING DEVICES

195 In this study, the optimization approach used in the hydraulic solver was expanded to handle  
196 control valves. Different approaches are used for the modeling of flow and pressure control  
197 valves. The headloss function of a flow control valve is adjusted by adding a penalty when  
198 the valve setting is violated. This modified headloss function is then treated like any other  
199 link in the hydraulic solver. Check valves are handled as special flow control valves with a  
200 minimum flow rate setting of zero. Pressure control valves are solved externally to the  
201 hydraulic solver by employing a Newton Projection Minimization algorithm, for which  
202 global convergence is guaranteed. The target flowrates and heads are subjected to constraints  
203 in the form of the conservation laws and the hydraulic behavior of elements in the system.

204

### 205 *Flow Regulating Devices*

206 Flow regulating valves include flow control valves that prevent the flow rate through the  
207 valve exceeding the target value, and non-return or check valves that allow flow to occur in  
208 only one direction. Flow control valves are modeled as part of existing links in the model,

209 since this results in a simpler model and avoids numerical problems in valves with very small  
 210 head losses.

211  
 212 In the proposed approach, the problem is not solved with hard inequality constraints (like in  
 213 Deuerlein *et al.*, 2009) but by adding penalties to the Content function. This exterior penalty  
 214 method facilitates the satisfaction of constraints while being robust and simple to implement.  
 215 The hydraulic solver used is based on an optimization approach, and this facilitates the  
 216 simultaneous handling of system links and flow control valves. The modified Content  
 217 optimization problem (2) now becomes:

$$218 \quad \min_{\mathbf{Q}} \tilde{f}(\mathbf{Q}, \mathbf{r}) = f(\mathbf{Q}) + \frac{1}{3} \sum_{j \in J_{FCV}} r_j \max(0, Q_j - Q_j^{set})^3$$

subject to  $-\mathbf{A}\mathbf{Q} - \mathbf{d} = 0_{nu}$

219 Where  $J_{FCV}$  is the index set of pipes with a flow control valve; the  $r_j$  are positive resistance  
 220 coefficients; and the last term penalizes violations of flow control valve settings. In general  
 221 the penalty function method requires that  $\tilde{f}(\mathbf{Q}, \mathbf{r}^k)$  is minimized for a sequence of  $\mathbf{r}^k$  until a  
 222 suitable solution is found. However, for this application it was found good results are  
 223 obtained with a large identical scalar  $r_{max}$  value. The corresponding headloss penalty is  
 224 obtained as:

$$225 \quad h_j^{FCV}(Q_j, r_{max}) = r_{max} \max(0, Q_j - Q_j^{set})^2 = h_0 \max\left(0, \frac{Q_j - Q_j^{set}}{\Delta Q}\right)^2 \quad (44)$$

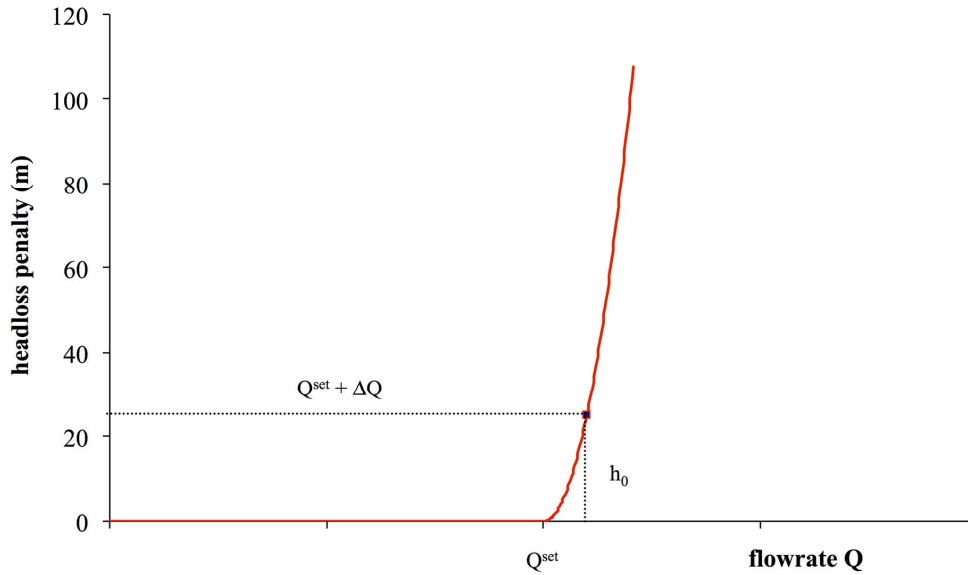
226 With  $h_0$  the headloss penalty for a flow rate violation of  $\Delta Q$ ;  $Q_j$  is the flowrate in the pipe  $j$ ;  
 227  $Q_j^{set}$  is the setting value; and  $\mathbf{h}^{FCV}$ , the headloss penalty function of  $\mathbf{Q}$ , is the gradient of the  
 228 additional term to the Content function.

229

**Code de champ modifié**  
**Mis en forme :** Police :12 pt, Ne pas vérifier l'orthographe ou la grammaire

230 The penalized headloss function for a flow control valve is a smooth quadratic function

231 whose general form is presented in **Figure 1**.



232

233 **Figure 1.** Headloss modeling of a flow control valve by external penalty.

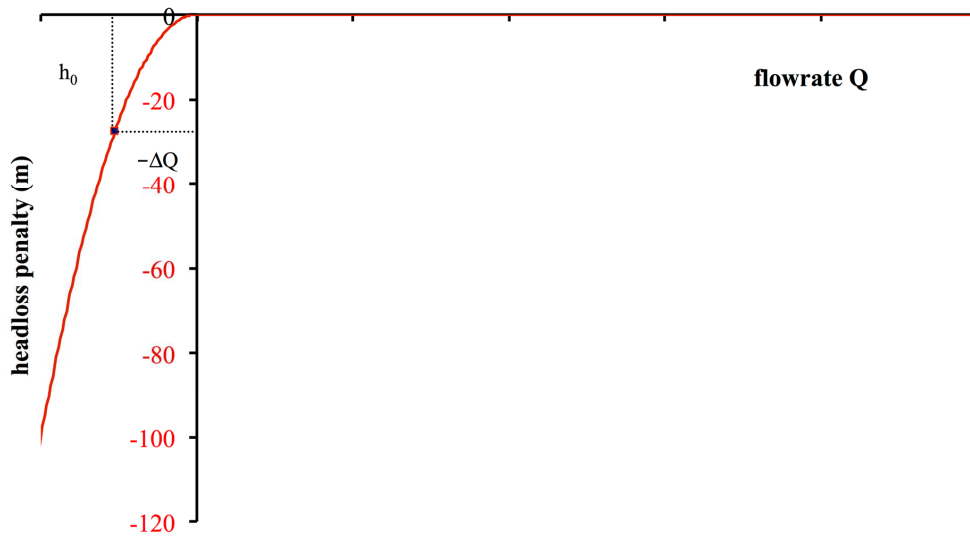
234 Check valves can be modeled by considering them as a special type of flow control valve

235 with the constraint that  $Q_k \geq 0$ . The penalty function for check valve is described by:

236 
$$h_k^{CV}(Q_k, r_{\max}) = -r_{\max} \max(0, -Q_k)^2 = -h_0 \max\left(0, \frac{-Q_k}{\Delta Q}\right)^2$$

Code de champ modifié  
 Mis en forme : Police :12 pt, Ne pas vérifier l'orthographe ou la grammaire  
 (55)

237 The corresponding curve is described in **Figure 2**.



238

239 **Figure 2.** Headloss modeling of a check valve by external penalty.

240 The generalized Content minimization problem for handling FCVs and CVs is then:

241

$$\min_{\mathbf{Q}} \tilde{f}(\mathbf{Q}, \mathbf{r}) = f(\mathbf{Q}) + \frac{1}{3} r_{\max} \left[ \sum_{j \in J_{FCV}} \max(0, Q_j - Q_j^{set})^3 + \sum_{k \in K_{CV}} \max(0, -Q_k)^3 \right]$$

subject to  $-\mathbf{A}\mathbf{Q} - \mathbf{d} = 0_{nu}$

(66)

Code de champ modifié

Mis en forme : Police :12 pt, Ne pas vérifier l'orthographe ou la grammaire

242

## 243 **Pressure Regulating Devices (PRDs)**

### 244 Formulation

245 A pressure-reducing valve (PRV) aims to maintain a certain maximum pressure on the  
 246 downstream side of the valve. PRVs are often used at the supply points of pressure zones to  
 247 ensure that pipes are not overloaded and leakage is minimized. On the other hand, a pressure-  
 248 sustaining valve (PSV) is used to maintain a minimum pressure on the upstream side of the  
 249 valve.

250  
251 Piller and Van Zyl (2009) used dummy pressure sustaining valves as a modeling trick to  
252 correct hydraulic predictions for network section supplied via a high-lying node experiencing  
253 negative pressure. This may occur if the normal supply pipe to the network section has  
254 failed. In practice, air will enter the system at the elevated node (*e.g.* through air valves, leaks  
255 or open taps), and thus the supply to the network section will likely be interrupted.

256  
257 Just like flow control valves, pressure regulating devices (PRDs) are modeled as part of  
258 existing links with a given target pressure on the downstream ( $i_D$ ) or upstream ( $i_U$ ) PRD sides.  
259 Thus for a PRV:

260 
$$H_{i_D} \leq H_{i_D}^{set}$$

261 and for a PSV:

262 
$$H_{i_U} \geq H_{i_U}^{set}$$

263 If  $\mathbf{S}$  is the selection matrix of the  $nt$  nodes with pressure setting targets, the complete set of  
264 constraints can be written in matrix form as:

265 
$$\mathbf{S}\mathbf{H} \leq \mathbf{H}^{set}$$

266 When in use, PRVs and PSVs create local headlosses to get the network pressures as close as  
267 possible to the head set point vector  $\mathbf{H}^{set}$  (target pressure + ground level). These local  
268 headlosses are added to the total headlosses  $\mathbf{h}(\mathbf{Q})$  for links with such devices:

269 
$$\mathbf{h}^{PRD}(\mathbf{Q}, \mathbf{r}) = \mathbf{B}(\mathbf{Q})\mathbf{r} \text{ with } \mathbf{B}(\mathbf{Q}) = \mathbf{C}\mathbf{S}_Q^T, r_i = \frac{8K_i}{g\pi^2 D_i^4}, i = 1, \dots, nt$$

(77)

Code de champ modifié

Mis en forme : Police :12 pt, Ne pas vérifier l'orthographe ou la grammaire

270 Where  $r_i$  is the secondary resistance factor of the pipe with  $K_i$  the dimensionless  
 271 corresponding secondary headloss coefficient,  $D_i$  the diameter of the pipe  $i$ ;  $C$  is the diagonal  
 272 matrix of element  $C_{ii} = \max(0, Q_i)^2$  and  $S_Q$  is the matrix of size  $n_t \times n_p$  for identifying the  
 273 pipes with PRVs. Control valves only act in one direction - depending on how they are  
 274 defined, these valves will either stop flow reversal, or, if negative flow is allowed, behave as  
 275 pipes with known secondary headloss coefficients.

276  
 277 Pressure regulating devices are handled with a function that penalizes deviations from the  
 278 target settings, as described by the first term in this function:

$$279 \quad \min_{\mathbf{r}} c(\mathbf{r}) = \frac{1}{2} (\mathbf{S}\mathbf{H}(\mathbf{r}) - \mathbf{H}^{set})^T \mathbf{I}^+ (\mathbf{S}\mathbf{H}(\mathbf{r}) - \mathbf{H}^{set}) + \frac{1}{2} m (\mathbf{r} - \mathbf{r}_0)^T \mathbf{I}^+ (\mathbf{r} - \mathbf{r}_0) \quad (8)$$

subject to:  $\mathbf{0}_{n_t} \leq \mathbf{r} \leq r_{\max} \mathbf{1}_{n_t}$

280 The second term in the equation is a Tikhonov regularization term used to ensure that  
 281 numerical problems are avoided in converging to a unique solution. The value of  $r_{\max}$  is the  
 282 same as that used for flow control valves:  $r_{\max} = h_0/\Delta Q^2$  in Figs. 1 and 2.  $\mathbf{I}^+$  is the indicator  
 283 matrix to implement the pressure control valve behavior for positive flowrates only,  $\mathbf{r}_0$  is the  
 284 value of  $\mathbf{r}$  from the previous iteration (or an initial estimate), and  $m$  is the Tikhonov factor  
 285 used to control the convexity of the function. The Tikhonov regularization term is only  
 286 included when the function has insufficient convexity, and in our experience it is mostly  
 287 equal to zero.

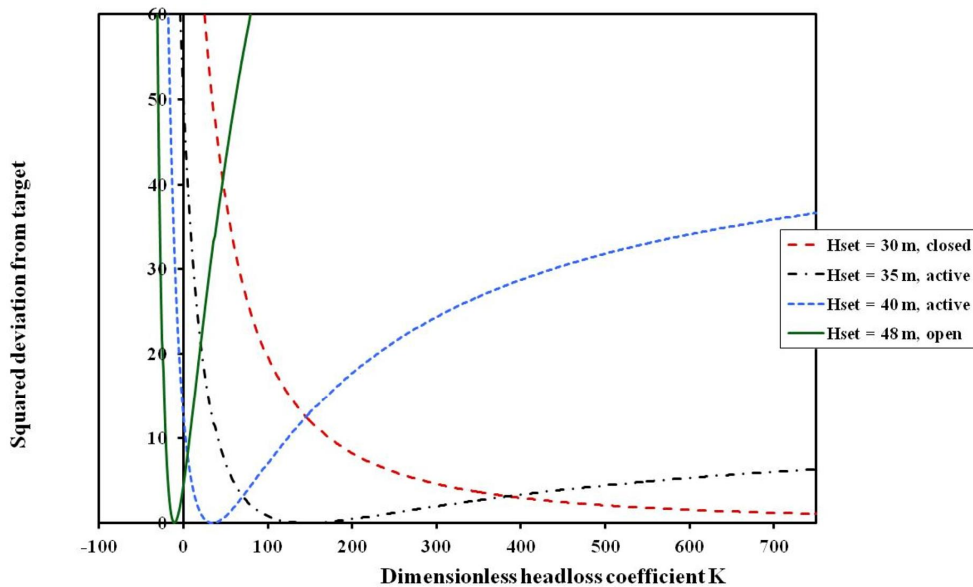
288  
 289 The function  $c$  is not differentiable at  $r_i$  such as  $Q_i(r_i) = 0$ . However, since control valves are  
 290 active in a very small positive range of  $Q_i$ , and is either open or closed outside this range, it  
 291 wasn't necessary to modify the  $\mathbf{I}^+$  term.

292

293 According to the Weierstrass theorem, there exists a solution for the problem by continuity of  
 294  $c$  on a non-empty compact (closed and bounded) constraint set. Because of a suitable  $m$   
 295 coefficient, the strict convexity of  $c$  guarantees the uniqueness of the solution.

296

297 For different pressure settings of a single PRV, [Figure 3](#) illustrates general form, in  
 298 relation to the  $K$  (dimensionless) coefficients, of the sum of squares of the residuals that are  
 299 obtained:



300

301 **Figure 33.** General form of criterion  $c(\cdot)$  to be minimized with  $m$  taken at zero.

302 For the four curves shown, the objective function  $c$  has a horizontal asymptote and a finite  
 303 limit when  $K$  tends to infinity. There is a head setting  $H^{set}$ , below which the objective  $c$  does  
 304 not have a minimum, in [Figure 3](#) when  $H^{set} \leq 30$  m. In such cases, the solution of (8)  
 305 is  $K_{max}$  if  $m = 0$  and correspondingly the valve status is "closed". For intermediary head  
 306 settings between 30 and 45 m, a minimum global solution exists in the first (positive)  
 307 quadrant, and the valve will be active if the strict inequality holds. For head setting values

Mis en forme : Anglais (États Unis)

Mis en forme : Anglais (États Unis)

Mis en forme : Anglais (États Unis)

Code de champ modifié

Mis en forme : Anglais (États Unis)

Mis en forme : Anglais (États Unis)

Mis en forme : Anglais (États Unis)

Mis en forme : Anglais (États Unis)

Mis en forme : Anglais (États Unis)



308 greater than or equal to 45 m, the valve status is  $\neq \text{open}$  and the unconstrained minimum  
309 occurs in the second (negative) quadrant. The solution of (8) for an open valve is  $K = 0$ . Note  
310 that the four curves are smooth, they each have no more than one minimum in the feasible  
311 set. From ~~Figure 3~~ Figure 3, it is clear that the criterion described by Eq. (8) without a  
312 regularization term (*i.e.*,  $m$  taken at zero) may be concave and its curve may possess inflexion  
313 points.

Mis en forme : Anglais (États Unis)

Mis en forme : Anglais (États Unis)

314

### 315 Optimality Criteria to determine the correct status of PRD valves

316 With the convexity and the differentiability of the least-squares criterion  $c$ , it is possible to  
317 define necessary and sufficient optimality conditions that are the associated Karush, Kuhn  
318 and Tucker (KKT) equations (a generalization of Lagrange condition for inequality  
319 constraints). These optimality conditions are useful to determine the correct **status** of the  
320 valves (rather than the valve settings). Once correct statuses of the PRD valves are  
321 determined, a second-stage least-squares problem Eq. (8) should be formulated with only the  
322 deviations from the target settings for PRDs that are active to determine the exact local head  
323 losses created by the control valves in order to meet the pressure targets.

324

325 To solve the KKT equations, the gradient of  $c$  has to be determined. Using the implicit  
326 function theorem, we can show that  $y = \mathbf{H}(\mathbf{r})$  is a continuous differentiable function with  
327 regards to the  $\mathbf{r}$  variables. This gives an expression for the gradient of  $c$ :

$$328 \quad \nabla c(\mathbf{r}) = \mathbf{J}^T (\mathbf{S}\mathbf{H}(\mathbf{r}) - \mathbf{H}^{set}) + m(\mathbf{r} - \mathbf{r}_0) \quad (9)$$

329 Where

$$330 \quad \mathbf{J} = \mathbf{S} \partial_{\mathbf{r}} \mathbf{H} = \mathbf{S} (\mathbf{A} \mathbf{D}^{-1} \mathbf{A}^T)^{-1} \mathbf{A} \mathbf{D}^{-1} \mathbf{B}$$

331 is the Jacobian matrix of the  $\mathbf{H}$  function at PRD target nodes with respect to the  $\mathbf{r}$   
 332 coefficients,  $\mathbf{B}$  is the same as in Eq. (7) and  $\mathbf{D}$  is the derivative of  $\mathbf{h}$  with respect to the flow  
 333 rate  $\mathbf{Q}$ . The total headloss function  $\mathbf{h}(\mathbf{Q},\mathbf{r})$  includes friction losses, FCVs, CVs and PRDs.  
 334 The calculation of the gradient of  $c$  is immediate, as the matrix to be inverted is very sparse  
 335 and its Cholesky decomposition is known from the current hydraulic solution of system (Eq.  
 336 1) with the previous values of  $\mathbf{r}$ .

337 Since  $c$  is continuously differentiable, and the constraints are linear, the first order KKT  
 338 optimality conditions are met (*e.g.*, see Bazaraa, 1993). Therefore there exist two positive  
 339 multiplier vectors  $\mathbf{M}^1$  and  $\mathbf{M}^2 \times \mathbf{0}_{nt}$  such that:

$$340 \quad \nabla c(\hat{\mathbf{r}}) = \mathbf{M}^1 - \mathbf{M}^2 \quad (10)$$

341 This consists of the Dual Feasibility conditions while

$$342 \quad (\mathbf{M}^1)^T \hat{\mathbf{r}} = 0 \text{ and } (\mathbf{M}^2)^T (\hat{\mathbf{r}} - r_{\max} \mathbf{1}_{nt}) = 0 \quad (11)$$

343 are the Complementary Slackness conditions with  $\hat{\mathbf{r}}$  being the optimal solution. The dual  
 344 feasibility condition states that the gradient is no longer sign-constrained.

345  
 346 These two conditions are used to check whether the KKT conditions have been met, *i.e.*  
 347 whether the correct solution for valve status has been found.

348  
 349 If  $r_i = 0$  (the  $i^{\text{th}}$  pressure control valve status is open), then by (11) it is necessary that  $M_i^2 = 0$   
 350 and Eq. (10) indicates that the  $i^{\text{th}}$  component of the gradient must be positive or zero. In  
 351 identical manner, if  $r_i = r_{\max}$  (the  $i^{\text{th}}$  pressure control valve status is closed), then  $M_i^1 = 0$  and  
 352 the corresponding gradient component must be negative or zero. Finally, if  $0 < r_i < r_{\max}$  (the  $i^{\text{th}}$

353 pressure control valve is active), then necessarily  $M_i^1 = M_i^2 = 0$  and the  $i^{\text{th}}$  gradient  
354 component should be zero.

355

### 356 Projected Levenberg-Marquardt Solution Algorithm

357 The solution method used is a slight modification of the Levenberg-Marquardt (LM)  
358 algorithm that accounts for all the constraints.

359

360 At the start of the solution algorithm, initial control valve statuses are obtained from the  
361 previous solution or initial settings. The system hydraulics is then solved, and the control  
362 valve  $\mathbf{r}$  resistances estimated with the iterative formula:

$$363 \quad \mathbf{r}^{i+1} = \mathbf{r}^i - \mathbf{P}_i \left[ \mathbf{J}_i^T \mathbf{J}_i + m \mathbf{I}_{nt} + e_i \text{diag}(\mathbf{J}_i^T \mathbf{J}_i) \right]^{-1} \nabla c^j \quad (12)$$

364 Where  $e_i$  is the LM damping factor,  $\mathbf{P}_i$  is the projection matrix for bounded primary  
365 constraints in (8) (i.e. valves that have fixed "closed" or "open" statuses). The value of  $e_i$  is  
366 increased if the primal feasibility conditions (PF) are not complied with, if  $\mathbf{J}_i^T \mathbf{J}_i$  is an ill-  
367 conditioned matrix or if there is no descent. In each step  $i$ , the hydraulic system is solved to  
368 determine  $\mathbf{Q}(\mathbf{r}^i)$  and  $\mathbf{H}(\mathbf{r}^i)$ . The operation of the pressure regulating devices is modeled by  
369 adjusting the local head loss coefficients to satisfy the optimality of a least squares problem.

370

371 The algorithm (Eq. (12)), which is a projected method on the box constraints of Eq. (8), will  
372 not change valves with status "open" or "closed" during iterations. A valve that is initially  
373 "active" may become "open" if  $K_i \leq 1E-3$  and "closed" if  $r_i \times r_{\max} \leq 1E-3 * r_{\max}$ .

374 The KKT conditions (Eqs. (10) and (11)) are checked after the iterative scheme Eq. (12) has  
375 converged. If all the Lagrange multipliers are non-negative, the KKT conditions are satisfied

376 and the first-step optimization of (8) can be terminated. If the KKT optimality conditions are  
377 not met, the pressure control valve with the most negative KKT multiplier is released, i.e. its  
378 status is changed from "non-active" (either "open" or "closed") to "active"

379  
380 Once the statuses of the PRD valves have been determined, a second-stage least-squares  
381 problem (Eq. (8)) is solved with the same constraints, but with deviations from the target  
382 settings only for "active" PRDs in the objective function: this is done to determine the exact  
383 local head losses created by active control valves in order to meet the pressure targets. This  
384 second-stage of the solution has to be done to remove any biases that fully open or closed  
385 valves have introduced in the solution.

386

### 387 **VALIDATION TESTS**

388 The proposed method was applied to a number of example networks:

389 - A simple network with a pressure-reducing valve on a pipeline between two tanks. This  
390 example was provided to illustrate the good convergence of the method when there is no  
391 interaction between valves.

392 - A simple network consisting of a flow control valve and a pressure-reducing valve in series  
393 on a pipeline between two tanks. This network posed a problem for early versions of Epanet.

394 - A simple network consisting of pressure-sustaining and pressure-reducing valves in series.  
395 This network poses a problem for the current version of Epanet.

396 - A simple network consisting of two valves in parallel that strongly interacts with each other.

397

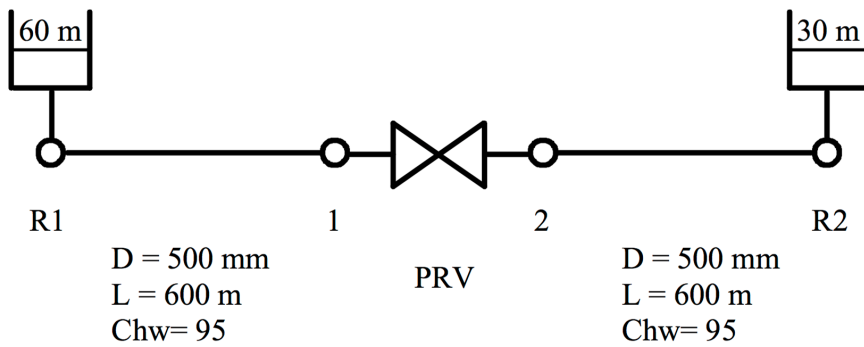
398 The simulation results are discussed with an emphasis on the convergence characteristics of  
399 the method.

400

401 **A PRV between two tanks.**

402 This example network is shown in [Figure 4](#) and was originally proposed by Simpson  
 403 (1999).

Mis en forme : Anglais (États Unis)  
 Mis en forme : Anglais (États Unis)



404  
 405 **Figure 44.** Network 1 with 1 PRV between two tanks.

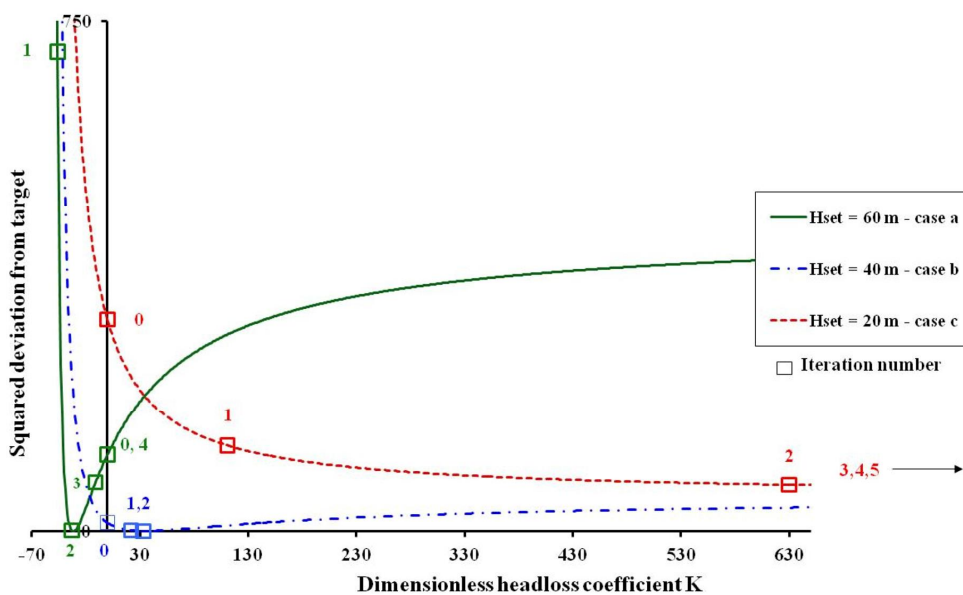
Mis en forme : Anglais (États Unis)  
 Code de champ modifié  
 Mis en forme : Anglais (États Unis)  
 Mis en forme : Anglais (États Unis)

406 The ground levels of nodes 1 and 2 are zero. Three target heads on node 2 were tested:  $H_{set} =$   
 407 a) 60 m, b) 40 m and c) 20 m. They correspond to the following three situations: a) valve  
 408 open and impossible to achieve the valve target setting because it is unrealistic for the  
 409 hydraulic grade line, b) device active (an equivalent local head loss is created with coefficient  
 410  $K^* = 34.5$ ), c) valve closed, target too low to achieve due to presence of tank R2. The three  
 411 situations are presented in [Figure 5](#). In all cases, the algorithm converges in no more  
 412 than 6 iterations.

Mis en forme : Anglais (États Unis)  
 Mis en forme : Anglais (États Unis)

413 **Situation a):** the initial solution is  $K^0 = 0$ . Next,  $K^1 = -46$  does not satisfy the non-negativity  
 414 constraint, therefore the damping parameter  $e_1$  in Eq. (12) is increased; the step size is  
 415 reduced and, for  $k = 4$ ,  $K^4$  is close to zero and the algorithm stops; gradient in Eq. (9) is  
 416 positive and has a value of  $\nabla c(0) = 2,547,090$ ; the Karush Kuhn and Tucker equations (10)  
 417 and (11) are satisfied.

418 **Situation b)**: As it is shown in [Figure 5](#), the algorithm is stabilized rapidly near the  
 419 true value; here, the direction of Levenberg-Marquardt is equivalent to the direction of the  
 420 Newton-Raphson method;  $e_i$  tends rapidly towards zero; the gradient is cancelled out.  
 421 **Situation c)**: the PRV is gradually closed to achieve the equivalent head loss of coefficient  
 422  $K^* = 483,738,332$  in 5 iterations; the gradient is cancelled out at this point, showing that it is  
 423 asymptotic on the x-axis at  $c(K)$ .



424  
 425 **Figure 5.** Algorithm performance at each iteration.

426 **A FCV and a PRV in series.**

427 The second example network shown in [Figure 6](#) was also proposed by Simpson  
 428 (1999). This network consists of a flow control valve (FCV) and a pressure-reducing valve in  
 429 series between two tanks. The tank T1 fills the tank T2 by gravity only. For non-valve  
 430 configurations (or equivalently the two control valves both inactive and having no minor  
 431 head losses), the flow rate and the piezometric head at the middle of the path would be  
 432 approximately 614 l/s and 45 m respectively. The FCV is made inactive (the flow set point is

Mis en forme : Anglais (États Unis)

Mis en forme : Anglais (États Unis)

Mis en forme : Anglais (États Unis)

Code de champ modifié

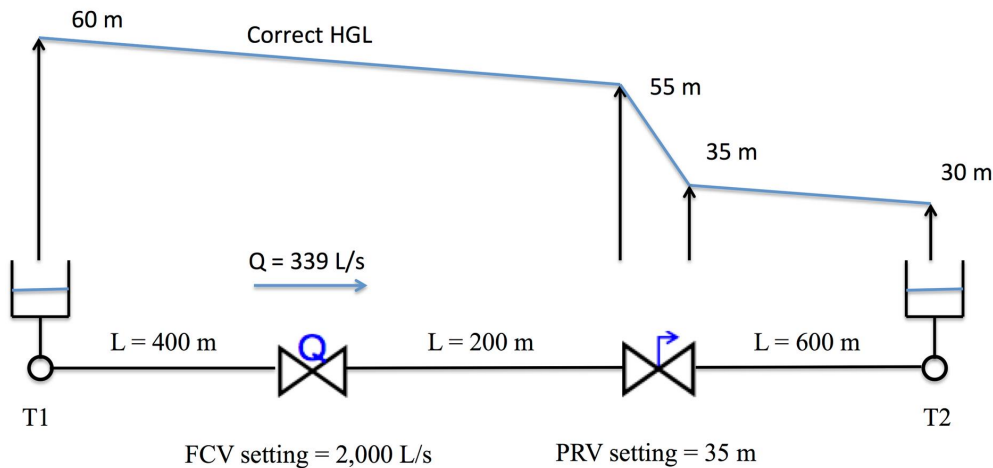
Mis en forme : Anglais (États Unis)

Mis en forme : Anglais (États Unis)

Mis en forme : Anglais (États Unis)

Mis en forme : Anglais (États Unis)

433 2,000 L/s) with a setting far in excess of the gravity flow rate. The PRV is operating and  
 434 yields a local headloss of 20 m with a dimensionless coefficient  $K^* = 131.7$ . The flow rate is  
 435 339 L/s. For the three pipes the diameter is 500 mm and the Hazen-Williams coefficient is  
 436 100. All the elevations at unknown head nodes are set to zero.



437

438 **Figure 66.** Network 2 with a FCV and a PRV in series between two tanks.

439 The main reason why previous versions of Epanet (e.g., version 2.00.10) may fail to converge  
 440 or converge to an incorrect solution, for this simple configuration with control valves is that  
 441 the algorithm may fail to determine the correct statuses of the valves. In the proposed  
 442 method, a continuous approach is used for both FCVs and PRDs. A flow control valve is  
 443 modeled as a local headloss that penalizes all violation of the flow set point. With this  
 444 approach a FCV and a PRV in series will pose no problem. The [Table 1](#) summarizes  
 445 the iterations of the Levenberg-Marquardt method for estimating the pressure valve settings.  
 446 With CV-Count is the number of pressure control valve components that has converged; RSS  
 447 is the residual sum of squares *i.e.*,  $c(K_i)$  with  $m=0$  ; GRAD/SD is the norm of the gradient  
 448 along the search direction; LM factor  $e_i$  is the Levenberg-Marquardt damping factor; and the  
 449 last column give the dimensionless friction factor that creates the local headloss  $0.5 K^* V^2/g$ .

450

Mis en forme : Anglais (États Unis)

Mis en forme : Anglais (États Unis)

Code de champ modifié

Mis en forme : Anglais (États Unis)

Mis en forme : Anglais (États Unis)

Mis en forme : Anglais (États Unis)

451

452

453 **Table 11. Convergence for the network with one FCV and one PRV in series.**

Iteration #	CV_Count	RSS	GRAD/SD	LM factor $\ell_i$	K PRV
0	0	50.00000	1881507.19753004	0.00010	0.00000
1	0	8.58045	269899.11571403	0.00004	40.19445
2	0	0.89534	40111.55927071	0.00002	88.28532
3	0	0.02955	4884.57232911	0.00000	122.05247
4	0	0.00006	206.63313520	0.00000	131.20525
5	0	0.00000	0.48852255	0.00000	131.67368
6	0	0.00000	0.00000380	0.00000	131.67480
7	1	0.00000	0.00000007	0.00000	131.67480

Mis en forme : Anglais (États Unis)

Code de champ modifié

Mis en forme : Anglais (États Unis)

454

455 The row iteration 0 corresponds to an initialization with  $K = 0$ , with the PRV assumed fully  
 456 open. The head at node 2 is  $H_2(K=0) = 45$  m, which is 10 m above the set point. The RSS is  
 457  $50 \text{ m}^2$ . The reductions of the RSS and of the Gradient are quadratic. The damping factor  $e_i$   
 458 decreases by 60 % at each iteration. Since there is no open or closed pressure control valve,  
 459 there is no need to solve the second-stage problem. Moreover, modeling flow control valves  
 460 with Eq. (4), penalizing the head loss if the flow setting is violated, requires no special  
 461 treatment for an open FVC. This is a clear advantage.

462

### 463 **A PSV and a PRV in series**

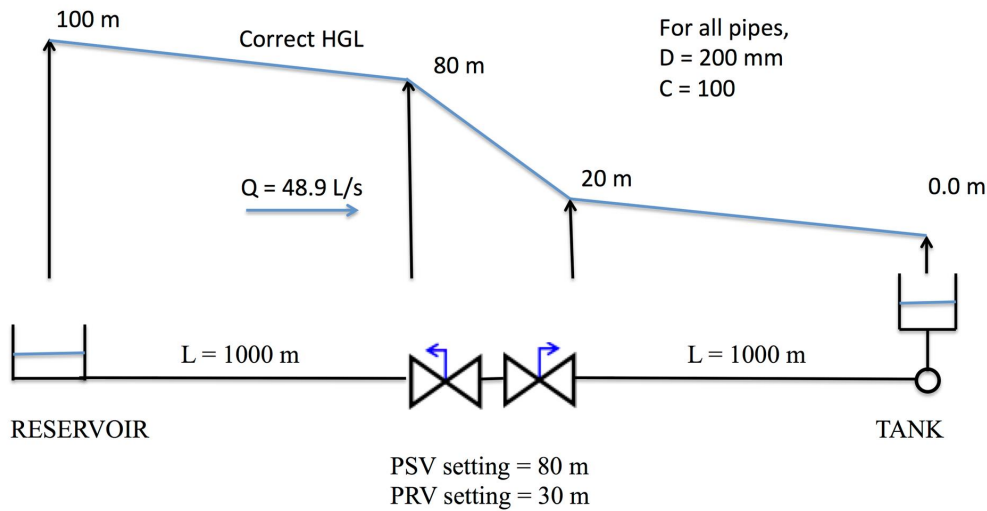
464 The third example network consists of two separate PSV and PRV in series as shown in  
 465 [Figure 7](#). Water flows from a reservoir to a Tank for a distance of 2 km. Halfway  
 466 between the reservoir and tank are two separate devices in series configured to model a  
 467 combination of pressure sustaining and pressure reducing (PSV/PRV) valves. The PSV/PRV

Mis en forme : Anglais (États Unis)

Mis en forme : Anglais (États Unis)



468 valve simultaneously controls the pressure on both sides, maintaining a certain minimum  
 469 pressure on the upstream side and another (lower) maximum pressure on the downstream  
 470 side. Both settings cannot be satisfied simultaneously and are active at different times of the  
 471 day. The initial level in the tank is zero. All elevations at junction nodes are zero. This simple  
 472 layout poses a problem in the latest version of Epanet (2.00.12). There is no convergence and  
 473 several warning are generated, such as "valve PSV causes ill conditioning" and "PSV open  
 474 but cannot deliver pressure at 0:00:00".



475  
 476 **Figure 7.** Network 3 with a PSV and a PRV in series between a reservoir and a tank.  
 477 At the end of the simulation run, the solution should be as shown in the **Figure 7**. The  
 478 PSV is active and yields a local headloss of 60 m with a dimensionless coefficient  $K^* =$   
 479 486.5. The PRV is open and the pressure at the downstream end of the valve is 10 m below  
 480 its setting. The flow rate is 48.9 L/s.  
 481 **Table 2** summarizes the iterations of the method (Eq. 12). It converges in 6 iterations  
 482 to a local minimum solution that is not the correct solution - the two valves both have head  
 483 losses of 25 m. The flow rate is 55.12 L/s, which is too high. Any additional simultaneous  
 484 valve closure will raise locally the least-squares criterion  $c$ . The pressure upstream the PSV is

Mis en forme : Anglais (États Unis)

Mis en forme : Anglais (États Unis)

Mis en forme : Anglais (États Unis)

Code de champ modifié

Mis en forme : Anglais (États Unis)

Mis en forme : Anglais (États Unis)

Mis en forme : Anglais (États Unis)

Mis en forme : Anglais (États Unis)

485 75 m (5 m below the setting). The pressure downstream the PRV is 25 m. The PRV is active  
 486 with a pressure constraint that is satisfied. This situation is not physically correct but can be  
 487 explained with the fact that the 2 valves interact strongly with each other.

488 **Table 22.** Initial convergence for the network with one PSV and one PRV in series.

Iteration #	CV_Count	RSS	GRAD/SD	LM factor $e_i$	K PSV	K PRV
0	0	649.75005	227019.02185376	0.00010	0.00000	0.00000
1	0	100.36013	33791.61183555	0.00004	75.35540	75.35540
2	0	28.46590	4479.20812686	0.00002	136.42557	136.42557
3	0	25.01620	265.86395946	0.00000	157.61510	157.61510
4	0	25.00000	1.40547468	0.00000	159.28421	159.28421
5	0	25.00000	0.00004447	0.00000	159.29323	159.29323
6	2	25.00000	0.00000079	0.00000	159.29323	159.29323

Mis en forme : Anglais (États Unis)

Code de champ modifié

Mis en forme : Anglais (États Unis)

489  
 490 To move the solution away from the local minimum solution, the recommended method is to  
 491 penalize the least-squares criterion with a Tikhonov term (Eqs. 8 and 12,  $m > 0$  and  $r_0 = 0$  for  
 492 the PRV). In addition the following rule is applied: after convergence, if a situation with  
 493 active or closed valve, but satisfied constraint occurs the valve with the highest residual is  
 494 opened. This applies with combined PSV/PRV valves but also to other valve configurations  
 495 with strong interaction.

496  
 497 The 6 first iterations are then followed by 6 further iterations with the PRV open as shown in

498 **Table 3.** The algorithm converges to the correct valve status solution (active PSV and  
 499 open PRV).

Mis en forme : Anglais (États Unis)

Mis en forme : Anglais (États Unis)

500  
 501 In addition, the solution at iteration 12 is equivalent to the solution at iteration 6: not only the  
 502 criterion cost  $RSS = 25 \text{ m}^2$  but also the hydraulic grade line with 75 m upstream the PSV, and

503 25 m downstream the PRV. The head loss of the PSV is 50 m with a dimensionless  
 504 coefficient  $K = 318.6$ , which is equal to the sum of the head losses in iteration 6. However,  
 505 the algorithm has to continue to the second stage to determine the correct setting of the PSV.  
 506 The RSS contribution for the PRV is removed from the total RSS as the valve is open. These  
 507 iterations are summarized in [Table 4](#).

508 **Table 33.** Valve status solution for the network with one PSV and one PRV in series.

Iteration #	CV_Count	RSS	GRAD/SD	LM factor $e_i$	K PSV	K PRV
7	0	90.32851	30282.48742520	0.00010	159.29323	0.00000
8	1	27.76165	3935.48041489	0.00004	277.43718	0.00000
9	1	25.01060	214.55220639	0.00002	315.86958	0.00000
10	1	25.00000	0.92318209	0.00000	318.57460	0.00000
11	1	25.00000	0.00002352	0.00000	318.58644	0.00000
12	2	25.00000	0.00002352	0.00000	318.58644	0.00000

Mis en forme : Anglais (États Unis)  
 Mis en forme : Anglais (États Unis)  
 Mis en forme : Anglais (États Unis)  
 Code de champ modifié  
 Mis en forme : Anglais (États Unis)

509  
 510 The exact setting of the PSV ( $K^* = 486.5$ ) is obtained after 6 additional iterations.

511 **Table 44.** Second-stage solving for the network with one PSV and one PRV in series.

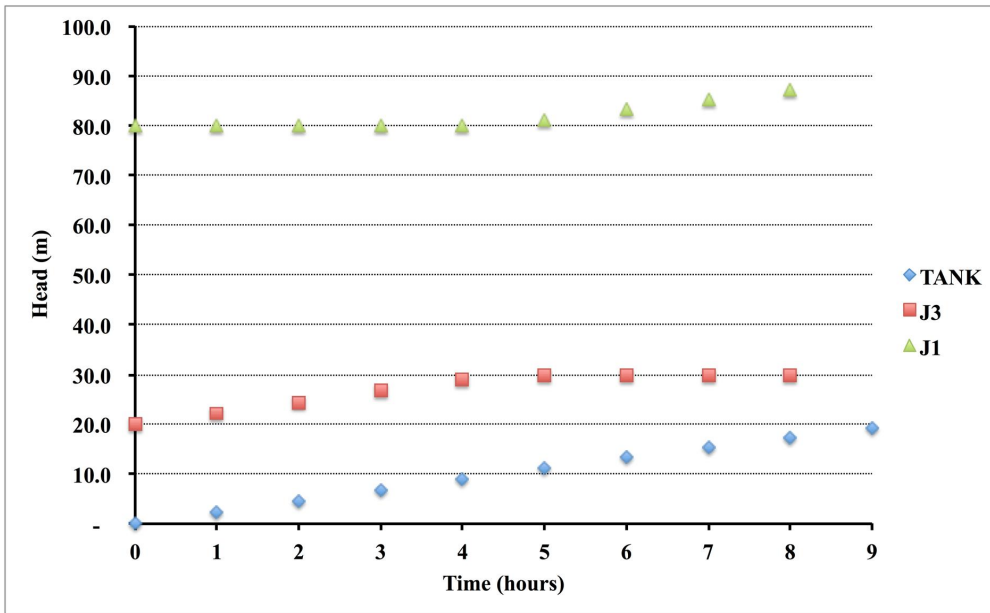
Iteration #	CV_Count	RESID_SS	GRAD/SD	LM factor $e_i$	K PSV
13	1	12.50000	3652.53528151	0.00010	318.58644
14	1	0.37937	434.37774607	0.00004	451.11238
15	1	0.00068	16.82032793	0.00002	484.93499
16	1	0.00000	0.03264390	0.00000	486.49091
17	1	0.00000	0.00000033	0.00000	486.49396
18	2	0.00000	0.00000033	0.00000	486.49396

Mis en forme : Anglais (États Unis)  
 Mis en forme : Anglais (États Unis)  
 Code de champ modifié

512  
 513 [Figure 8](#) shows the nodal heads for the 9 first hours. The tank is cylindrical with 20  
 514 m for the maximum level and 10 m for the diameter. J1 is a junction node just upstream the  
 515 PSV and J3 another one just downstream the PRV. The tank level was updated every hour

Mis en forme : Anglais (États Unis)  
 Mis en forme : Anglais (États Unis)

516 using the forward Euler method. It may be seen than for the first 4 hours the PSV is operating  
 517 and the PRV is open. Then, starting from time = 5 h the PSV is open and the PRV is active.  
 518 The 9-hour simulation requires a total of 112 iterations.



519  
 520 **Figure 88.** Head time series for selected nodes in network 3.

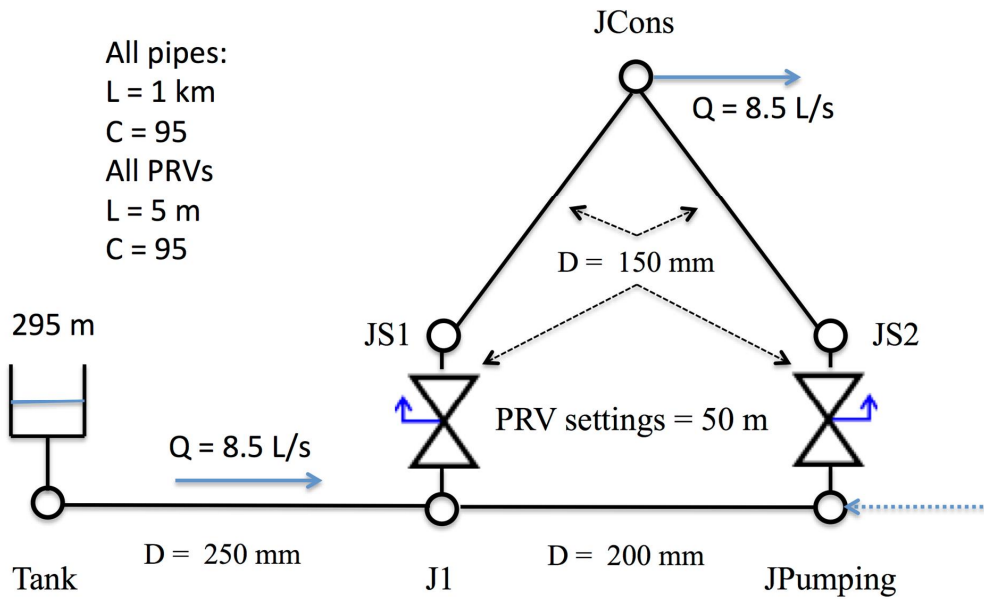
521 **Two PRVs in parallel.**

522 The fourth example network consists of two PRVs in parallel as shown in [Figure 9](#) ~~Figure 9~~.  
 523 The system uses a tank or a pumping station to supply consumers at node JCons. When the  
 524 pumps are operating the tank is filling through a top inlet. When the pumps are switched off,  
 525 the tank supplies water to the system. The latter situation is represented in [Figure 9](#) ~~Figure 9~~.  
 526 Water flows from the tank to node J1. Then, the flow separates in two different paths with a  
 527 PRV on each. The PRVs are situated 1 km upstream the node JCons. The pressure settings  
 528 are 50 m for both PRVs. All node elevations are 200 m. The level in the Tank is 3m above its  
 529 bottom level of 292 m. The lengths of all three pipes are 1,000 m and their Hazen-Williams  
 530 coefficients are 95. The demand at JCons is 8.5 L/s.

Mis en forme : Anglais (États Unis)  
 Mis en forme : Anglais (États Unis)  
 Mis en forme : Anglais (États Unis)  
 Code de champ modifié

Mis en forme : Anglais (États Unis)  
 Mis en forme : Anglais (États Unis)

Mis en forme : Anglais (États Unis)  
 Mis en forme : Anglais (États Unis)



531

532 **Figure 99.** Network 4 with two PRVs in parallel.

533 The [Table 5](#) summarizes the iterations of the Levenberg-Marquardt method. It  
 534 converges in 12 iterations to a global optimum (RSS = 0.). It may be seen that at iterations 2  
 535 and 3 the damping factor  $e_i$  has been multiplied by ten. This was done to correct the search  
 536 direction in order to have an effective descent for the RSS criterion. The two valves are  
 537 operating and produce a local head loss of 44.71 m for PRV1, and 44.47 m for PRV2. The  
 538 difference 0.24 m corresponds to the linear head loss of the 1 km long pipe J1/JPumping. A  
 539 flow rate of 4.25 L/s flows through this pipe. The dimensionless coefficients are relatively  
 540 large:  $K^*_{PRV1} = 15,164$  and  $K^*_{PRV2} = 15,083$ . These two valves are strongly linked, which  
 541 plays a role for the weaker, linear convergence rate.

542

543

544

545

- Mis en forme : Anglais (États Unis)
- Mis en forme : Anglais (États Unis)
- Code de champ modifié
- Mis en forme : Anglais (États Unis)
- Mis en forme : Anglais (États Unis)
- Mis en forme : Anglais (États Unis)

546 **Table 55.** Convergence for the network with two PRVs in parallel.

Iteration #	CV_Count	RSS	GRAD/SD	LM factor $e_i$	K PRV1	K PRV2
0	0	1988.96816	1185.48303586	0.00010	0.00000	0.00000
1	0	0.01086	0.26839385	0.00004	13517.19639	17036.82993
2	0	0.17871	0.26839385	0.00040	13517.19639	17036.82993
3	0	0.04189	0.26839385	0.00400	13517.19639	17036.82993
4	0	0.00772	0.32911957	0.00160	13763.48414	16695.22089
5	0	0.00463	0.89014765	0.00064	14189.38031	16134.05340
↓						
12		0.00000	0.00000000	0.00000	15164.07956	15083.08428

Mis en forme : Anglais (États Unis)

Code de champ modifié

Mis en forme : Anglais (États Unis)

Mis en forme : Anglais (États Unis)

547

548 The residual Jacobian matrix  $J$  at iteration 10 is as follows:

549 
$$\mathbf{J} = \begin{pmatrix} 163.1268 & 163.0637 \\ 163.0637 & 163.2535 \end{pmatrix}$$

550 It may be seen than the 2 PRVs influence each other to the same extent and when one of  
 551 PRVs experiences a small change, a similar change is expected in the other valve.

552

553 **CONCLUSION**

554 A new method is presented for handling control valves (including check valves) in hydraulic  
 555 network modeling. In this method, the behavior of check and control valves are described by  
 556 continuous functions rather than the mixed discrete-continuous formulation commonly used.

557

558 In this method, flow control valves are handled by imposing a penalty on the valve's headloss  
 559 function when the flow setting is violated. Check valves are modeled as special flow control  
 560 valves with a minimum flow rate setting of zero. The modified headloss functions for flow  
 561 control valves are incorporated into the hydraulic network equations and the resulting

562 governing equations are solved using a standard solver algorithm. In this work, a Lagrange-  
563 Newton-type algorithm by Piller (1995) was used.

564

565 Pressure control valves (such as pressure reducing and pressure sustaining valves) are  
566 handled externally to the hydraulic solver through an optimization routine. The goal of the  
567 optimization is to find the secondary loss coefficients of the pressure control valves that will  
568 minimize the differences between the nodal and the target pressures.

569

570 The proposed method has several benefits compared to the current discrete-continuous  
571 formulation. The derivatives of the heads in relation to the input parameters can be written  
572 explicitly as functions of the flow rates, and the gradients of the functions with respect to the  
573 optimization variables can be obtained analytically. This, in conjunction with the fact that  
574 only linear constraints are required in the optimization process, provides good conditions for  
575 fast convergence of the method. The robustness of the optimization is ensured by using a  
576 Levenberg-Marquardt projection minimization algorithm, for which global convergence is  
577 guaranteed.

578

579 It is shown with several case studies that the method finds interesting solutions to control  
580 valve problems without resorting to modeling tricks. It is proved to be efficient on  
581 problematic case studies.

582

583 While only control valves were considered in this paper, variable speed pumps and handling  
584 of high-lying nodes with negative pressures (Piller and Van Zyl 2009) can also be included in  
585 the proposed algorithm.

586

587 **REFERENCES**

- 588 Bazaraa, M. S., Sherali, H. D., and Shetty, C. M. (1993). « Nonlinear Programming - Theory  
589 and Algorithms. », Wiley, 638 p, second edition.
- 590 Carpentier, P., Cohen, G., and Hamam, Y. (1985). "Water Network Equilibrium, Variational  
591 Formulation and Comparison of Numerical Algorithms." EURO VII, Bologna, IT.
- 592 Chandrashekar, M., and Stewart, K. H. (1975). "Sparsity Oriented Analysis of Large Pipe  
593 Networks." Journal of the Hydraulics Division, 101(HY4), 341-355.
- 594 Collins, M., Cooper, L., Helgason, R., Kennington, R., and Leblanc, L. (1978). "Solving the  
595 Pipe Network Analysis Problem using Optimization Techniques." Management  
596 Science, 24(7), 747-760.
- 597 Cross, H. (1936). "Analysis of Flow in Networks of Conduits or Conductors." Bulletin No.  
598 286, University of Illinois Engineering Experimental Station.
- 599 Deuerlein, J., Cembrowicz, R. G., and Dempe, S. (2005). "Hydraulic Simulation of Water  
600 Supply Networks Under Control." World Water and Environmental Resources  
601 Congress (EWRI05), Anchorage (AK), US, printed by ASCE.
- 602 Deuerlein, J., Simpson, A., R., and Gross, E. (2008). "The Never Ending Story of Modeling  
603 Control-Devices in Hydraulic Systems Analysis." 10th International Water  
604 Distribution System Analysis conference (WDSA), 17-20 August 2008, Kruger  
605 National Park, ZAF, printed by ASCE, Volume 340/, 72.
- 606 Deuerlein, J., W., Simpson, A., R. , and Dempe, S. (2009). "Modeling the Behavior of Flow  
607 Regulating Devices in Water Distribution Systems Using Constrained Nonlinear  
608 Programming." Journal of Hydraulic Engineering, 135(11), 970-982.
- 609 Epp, R., and Fowler, A. G. (1970). "Efficient Code for Steady-State Flows in Networks."  
610 Journal of the Hydraulics Division, 96(HY1), 43-56.



- 611 Lam, C. F., and Wolla, M. L. (1972). "Computer Analysis of Water Distribution Systems:  
612 Part II - Numerical Solution." Journal of the Hydraulics Division, 98(HY3), 447-460.
- 613 Martin, D. W., and Peters, G. (1963). "The Application of Newton's Method to Network  
614 Analysis by Digital Computer." Journal of the Institute of Water Engineers, 17, 115-  
615 129.
- 616 Ortega J.M. and Rheinboldt W.C. (1970). Iterative solution of nonlinear equations in  
617 several variables. Computer Science and Applied Mathematics, Academic  
618 Press,1970.
- 619 Piccolo, Safège (2014). <http://www.safège.com/en/innovation/modelling/piccolo/> (accessed on  
620 21 July 2014).
- 621 Piller, O. (1995). "Modeling the behavior of a network - Hydraulic analysis and sampling  
622 procedures for parameter estimation." PhD thesis in Applied Mathematics from the  
623 Mathematics and Computer Science Doctoral School at the University of Bordeaux  
624 (PRES), defended on 03 February 1995, 288 pages, Talence, France.
- 625 Piller, O., and Brémond, B. (2001). "Modeling of Pressure Regulating Devices: A Problem  
626 now Solved." World Water & Environmental Resources congress, EWRI01, Orlando  
627 (FL), US, printed by ASCE.
- 628 Piller, O., Gancel, G., and Propato, M. (2005). "Slow Transient Pressure Regulation in Water  
629 Distribution Systems." Eight International Conference on Computing and Control in  
630 the Water Industry CCWI05 Water Management for the 21st Century, University of  
631 Exeter, UK, printed by Centre for Water Systems, Volume 1/2, 263-268.
- 632 Piller, O., and van Zyl, J. E. (2009). "Pressure-Driven Analysis of Network Sections Supplied  
633 Via high-lying Nodes." Computing and Control in the Water Industry 2009  
634 'Integrating Water Systems', The Edge, University of Sheffield, printed by CRC  
635 press/Balkema, Volume 1/1, 257-262.

Code de champ modifié

- 636 Porteau, Cemagref (2014). <http://porteur.irstea.fr/>, (accessed on 21 July 2014).
- 637 Rossman, L. A. (2000). "EPANET User's manual." U.S. Environmental agency, Cincinnati,  
638 Ohio.
- 639 Simpson, A. (1999). "Modeling of Pressure Regulating Devices: The last major Problem to  
640 be Solved in hydraulic Simulation." Water Resources Planning and Management  
641 Conference, Tempe (AZ), US, printed by ASCE, 9p.
- 642 Todini, E., and Pilati, S. (1988). "A Gradient Projection Algorithm for the Analysis of Pipe  
643 Networks." Computer Applications for Water Supply and Distribution, Leicester  
644 Polytechnic, printed by Research Study Press Ltd., Volume 1/1.
- 645 Wood, D. J., and Charles, C. O. A. (1972). "Hydraulic Network Analysis Using Linear  
646 Theory." Journal of the Hydraulics Division, 98(HY7), 1157-1170.
- 647

Code de champ modifié

648 **LIST OF FIGURE CAPTIONS**

649 **Figure 1.** Headloss modeling of a flow control valve by external penalty. \_\_\_\_\_ 11  
650 *Figure 2.* Headloss modeling of a check valve by external penalty. \_\_\_\_\_ 12  
651 *Figure 3.* General form of criterion  $c(K)$  to be minimized with  $m$  taken at zero. \_\_\_\_\_ 15  
652 *Figure 4.* Network 1 with 1 PRV between two tanks. \_\_\_\_\_ 20  
653 *Figure 5.* Algorithm performance at each iteration. \_\_\_\_\_ 21  
654 *Figure 6.* Network 2 with a FCV and a PRV in series between two tanks. \_\_\_\_\_ 22  
655 *Figure 7.* Network 3 with a PSV and a PRV in series between a reservoir and a tank. \_\_\_\_\_ 24  
656 *Figure 8.* Head time series for selected nodes in network 3. \_\_\_\_\_ ~~27~~26  
657 *Figure 9.* Network 4 with two PRVs in parallel. \_\_\_\_\_ ~~28~~27

658

659 **LIST OF TABLE CAPTIONS**

660 *Table 1.* Convergence for the network with one FCV and one PRV in series. \_\_\_\_\_ ~~22~~23  
661 *Table 2.* Initial convergence for the network with one PSV and one PRV in series. \_\_\_\_\_ 25  
662 *Table 3.* Valve status solution for the network with one PSV and one PRV in series. \_\_\_\_\_ 26  
663 *Table 4.* Second-stage solving for the network with one PSV and one PRV in series. \_\_\_\_\_ 26  
664 *Table 5.* Convergence for the network with two PRVs in parallel. \_\_\_\_\_ 29

665

666